# INVESTIGATION ON THE RELATION BETWEEN PHYSICAL AND RADIOMETRICAL PROPERTIES OF SNOW COVERS

*Roberto Salzano[1], Rosamaria Salvatori[1] and Florent Dominé[2]*

1. CNR, Institute for Atmospheric Pollution, Monterotondo (Rome), Italy; {salzano / salvatori}(at)iia.cnr.it
2. CNRS, Laboratoire de Glaciologie et Géophysique de l'Environment, Saint Martin d'Hères cedex, France; florent(at)lgge.obs.ujf-grenoble.fr

## ABSTRACT

The extension of the snow cover and the distribution of different snow types can be considered an indicator of global changes and a key parameter in the global radiation balance of the Earth. Moreover, in the mountain regions the possibility to monitor the snow characteristics using remote sensing images can support hydrological studies. The reflectance of snow is determined in part by the size and shape of snow crystals, especially in the short wave infrared (SWIR) wavelength region; for this reasons it is possible to use remote sensed images to map differences in the snow cover. The Specific Surface Area (SSA) of snow is a crucial variable for understanding snow chemistry and air snow exchanges of chemical species that can also be related to snow reflectance. This study shows how field spectral measurement and SSA data of snow samples can be used as input data for classifying Landsat TM SWIR images in order to obtain maps of different snow types. This method can be a very useful tool to monitor the snow metamorphism, air-snow exchanges and climate.

**Keywords:** snow reflectance, SSA, Landsat.

## INTRODUCTION

The extent of the snow cover is a key parameter for global change studies as well as for hydrological balance calculation in alpine regions; snow cover extent monitoring can be performed using remote sensed images and field data (1,2,3). Satellite images, collected in the wavelength range 400-2500 nm, can be used in order to provide reliable cartography of snow surfaces, but some physical characteristics of the snow must be taken into account. Snow is a highly unstable target and structural changes of grain size and shape may occur quite rapidly due to climate and atmospheric variations. Even if the spectral contrast between snow and ice is such that these surfaces can be easily mapped, the same contrast between different snow surfaces can be very subtle. Snow reflectance is due to its light scattering properties, that are a function of the size and shape of snow grains and to the absorption by the ice medium and to the presence of impurities (4). In the visible range, ice is a weak absorber, and its reflectance is not very sensitive to its physical properties but is largely dependent on its impurity content such as soot particles. In the wavelength range 1.5 to 2.5 μm, ice is a strong absorber and its albedo is very strongly determined by the size and shape of snow grains, while being insensitive to impurities (5). The description of the effect of crystal size and shape on snow optical properties is an enormous task (6), and an approximation has been proposed (7): snow crystals are considered to be spheres of equivalent surface to volume ratio ($S/V$). The benefit of this approach is that the equivalent-sphere size of snow crystals is the main physical variable that affects snow scattering properties, shape being often secondary.

To understand snow cover variability, it also necessary to understand chemistry and air–snow exchanges of chemical species (8); this can be done measuring the specific surface area (SSA) of snow. The specific surface area ($SSA$) of snow is defined as the surface area of snow crystals that is accessible to gases per unit mass and it is proved that the $SSA$ decreases during snow metamorphism as grain size increases.

Since it has been shown that the scattering fraction of snow reflectance could be modelled in an acceptable manner by spheres of equal $S/V$, there is a clear link between reflectance $\rho$ and snow surface area: $SSA = S/(V \cdot \rho)$.

In the SWIR region, impurities have little effect, and reflectance is determined by scattering where the relation with *SSA* is much simpler than that in the visible. By simultaneously measuring the *SSA* and the reflectance of snow at Ny-Ålesund (Svalbard, Norway), *SSA* is found to be the main physical factor responsible for the reflectance variations in the SWIR (9).

Following this consideration, in this paper we present a preliminary study in which Landsat infrared images of the Brøggen peninsula (Svalbard) were processed, taking into account field spectroradiometric data and laboratory *SSA* measurements in order to obtain a distribution map of different *SSA* value in the studied area.

## FIELD AND LABORATORY DATA

Field data were acquired near Ny-Ålesund, between 21 April and 7 May 2001. The measurements were performed under clear sky conditions, with occasionally few scattered clouds far from the sun.

In the field survey the following data were recorded:

- snow data, particularly referred to grain shape and size in the first 10 cm of the snow pack;
- reflectance curves in the 350-2500 nm wavelength range;
- climatic data such as air temperature, cloud cover, wind speed;
- other ancillary data such as GPS coordinates and description of the investigated sites.

Measurements of the snow reflectance were carried out with a portable spectroradiometer (FieldSpec, Analytical Spectral Devices, Boulder, CO, USA), that allows reflectance data in the 350-2500 nm spectral range to be acquired by three separate spectrometers, that operate in the ranges 350-1050 nm, 900-1850 nm and 1700-2500 nm, with 10 nm resolution.

Fieldspec automatically calculates the reflectance value as the ratio between the incident solar radiation reflected from the surface target and the incident radiation reflected by a reference white Spectralon® panel, to be regarded as a Lambertian reflector. For this research work a bare fiber optics with a FOV of 25° was used, thus yielding a surface area of about 4 $cm^2$ when the instrument is about 10 cm above the target. Special care was taken that the radiometer was nadir viewing over the surveyed surface. All measurements were carried out between 12:00 and 15:00 local time, when the solar zenith angle was between 64 and 68°.

*Table 1: Description of sampled sites and conditions during the field survey carried out in 2001 under clear sky condition.*

| Sample N° | Date | time | Sun elevation ° | Lat. | Long. | Elevation m a.s.l. | Air T °C |
|---|---|---|---|---|---|---|---|
| 1 | 21/4 | 12:15 | 23 | 78°56.91' N | 11°44.88' E | 45 | -11.6 |
| 2 | 23/4 | 13:00 | 23 | 78°55.29' N | 11°56.75' E | 7 | -8.0 |
| 3 | 26/4 | 12:30 | 24 | 78°47.24' N | 13°03.17' E | 464 | -1.0 |
| 4 | 28/4 | 13:00 | 24 | 78°50.95' N | 11°54.21' E | 5 | -0.5 |
| 5 | 28/4 | 13:10 | 24 | 78°51.80' N | 11°39.01' E | 210 | -1.0 |
| 6 | 03/5 | 12:30 | 26 | 78°53.59' N | 11°50.19' E | 190 | -2.6 |
| 7 | 03/5 | 13:30 | 25 | 78°47.24' N | 12°04.61' E | 240 | -1.0 |
| 8 | 03/5 | 15:00 | 22 | 78°45.80' N | 12°11.39' E | 370 | -1.0 |
| 9 | 04/5 | 12:40 | 26 | 78°55.45' N | 11°55.67' E | 5 | -1.0 |

The absolute reflectance was obtained by multiplying this reflectance factor by the reflectance spectrum of the panel. The measurement conditions were determined according to (10) and the estimated error of absolute reflectance was about 2%. Twenty to 30 measurements were carried out for every target, and each measurement represented an integration of 50 acquisition cycles.

Snow Surface Area (*SSA* i.e. the surface area of the actual sample, expressed in $cm^2$ per unit mass of sample) was measured in a cold room using a volumetric method with Brunnauer, Emmet and Teller (BET) analysis (11). Briefly, the principle of the method is to determine the number of $CH_4$ molecules that can be adsorbed on the snow surface. In practice, the adsorption isotherm of $CH_4$ on the snow has to be recorded. A BET analysis is then used to obtain the surface area (SA) from the isotherm. The snow mass was determined by weighing, and the SSA was derived as the ratio of SA over mass. The method has a 6% reproducibility and a 12% accuracy. The snow samples studied and the data obtained are summarised in Tables 1 and 2.

*Table 2: SSA and field reflectance ([a] replicated measurements) sampled in the TM wavelength range.*

| Snow type | Sample N° | SSA $cm^2/g$ | density $g/cm^3$ | Reflectance TM4 | TM5 | TM7 |
|---|---|---|---|---|---|---|
| Fresh dendritic snow | 1 | 683 | 0.013 | 0.824 | 0.2030 | 0.1708 |
| Needles and dendrites | 2 | 447 | 0.16 | 0.878 | 0.1427 | 0.1128 |
| Surface wind crust | 3 | 304 | 0.34 | 0.853 | 0.1055 | 0.0816 |
| Deep faceted crystals | 4 | 145 | 0.22 | 0.809 | 0.0347 | 0.0259 |
| Deep faceted crystals | [a]5 | 145 | 0.21 | 0.767 | 0.0372 | 0.0272 |
| | | 145 | | 0.779 | 0.0306 | 0.0190 |
| Deep faceted crystals | 6 | 120 | 0.27 | 0.852 | 0.0313 | 0.0231 |
| Rounded crystals, a few facets | 7 | 124 | 0.33 | 0.859 | 0.0362 | 0.0257 |
| Deep faceted crystals | 8 | 89 | 0.32 | 0.789 | 0.0158 | 0.0103 |
| | | 102 | | 0.822 | 0.0211 | 0.0135 |
| Depth hoar | [a]9 | 102 | 0.25 | 0.799 | 0.0209 | 0.0136 |
| | | 102 | | 0.790 | 0.0268 | 0.0184 |
| | | TM band (nm) | | 760 - 900 | 1550 - 1750 | 2080 - 2350 |

Figure 1 shows the spectral reflectance of three snow samples, and illustrates that the SWIR reflectance is related to SSA, while no obvious relationship appears in the visible.

The linear correlation coefficient, $R^2$, is always greater than 0.9 from 1100 nm to 2500 nm, where the radiometric properties are mainly affected by snow crystal size. In order to compare the SSA values with reflectance data deriving from the images, the correlation coefficients were also calculated taking into account mean reflectance values computed, using a squared function, in the wavelength ranges corresponding to Landsat Thematic Mapper bands. As expected from the plot in Figure 2, the correlation in the TM visible bands is very low, while it is greater than 0.98 in the ranges of TM5; increasing to 0.99 at TM7 range. Given the number of data points, all of these values indicate correlations significant at levels $p<0.01$.

This result clearly suggests that it may be possible to determine snow *SSA* from its reflectance at a single wavelength, or even over an optical band of limited width. Therefore it was possible to express the relation between reflectance in band TM5 and TM7 as follows (Figure 3):

TM5 $$SSA = 3054.2 \cdot \text{Reflectance}_{TM5} + 30.083 \qquad R^2 = 0.986 \qquad (1)$$

TM7 $$SSA = 3620.1 \cdot \text{Reflectance}_{TM7} + 47.125 \qquad R^2 = 0.990 \qquad (2)$$

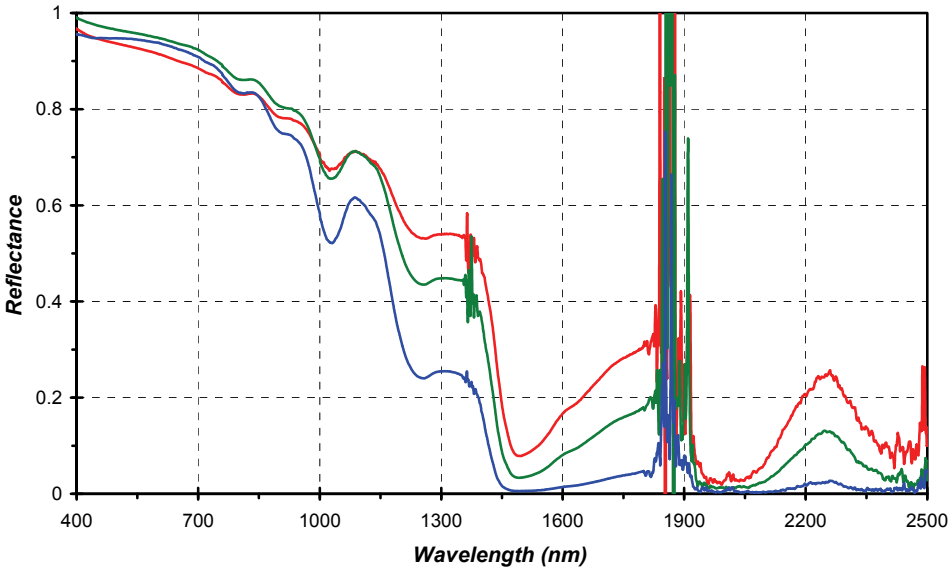


*Figure 1: Spectral reflectance of three snow samples (red – 1; green – 3; blue – 9; respectively in Table 2), illustrating the effect of snow SSA on reflectance in the IR, and the lack of effect in the visible.*

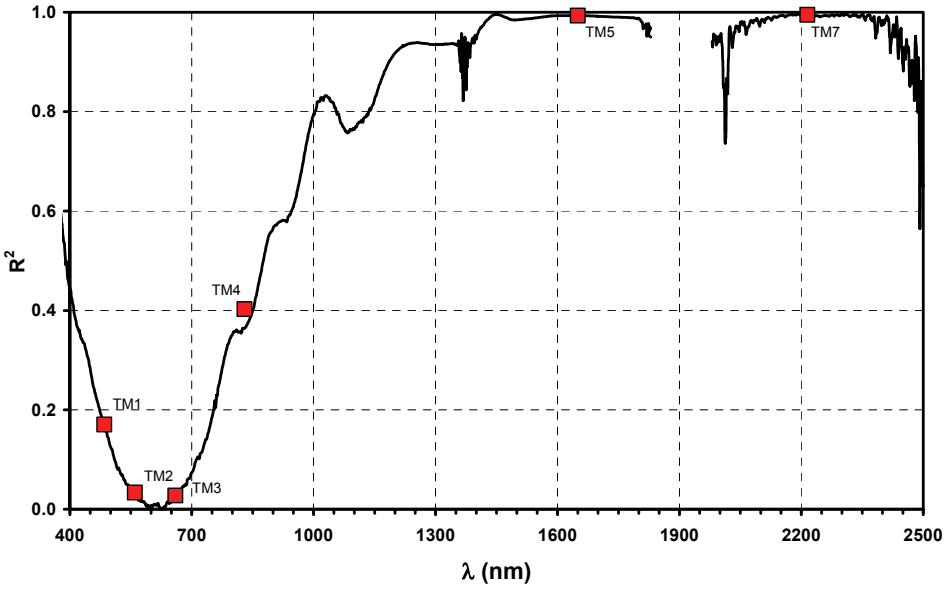


*Figure 2: Correlation between SSA and field reflectance measured at Ny-Ålesund, red squares show the TM spectral range.*

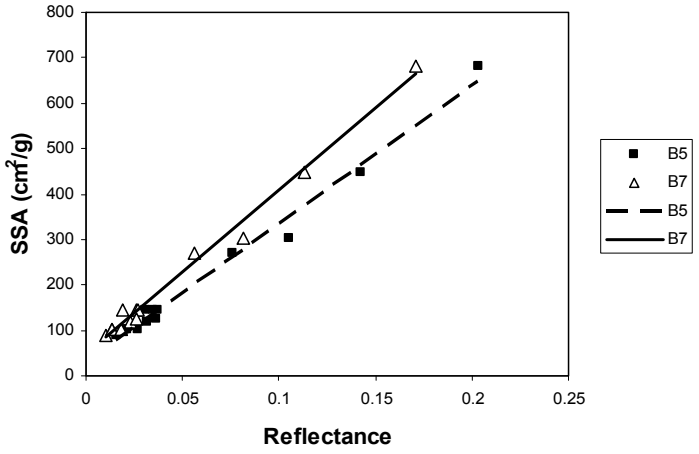


*Figure 3: Relationship between SSA and reflectance calculated for TM bands 5 and 7.*

## IMAGE PROCESSING

A Landsat Thematic Mapper image of 26 April 1998 was acquired, and radiometric calibration using ENVI routine (12) was performed in order to obtain reflectance values from DN values. TM5 and TM7 bands were corrected using "dark object" correction, considering sea water as valid dark object for these wavelength ranges (13). The reflectance values, derived from the images, were compared with spectroradiometric data collected in the same region on flat areas during the snow surveys carried out on 26 April 1998 (14). The good agreement between image-reflectance values and field-reflectance values suggests that further atmospheric and geometric corrections are not necessary.

Using the relation between reflectance and SSA for band TM5 and TM7 (Figure 3 and Eq. (1) and (2)) the reflectance values of TM5 and TM7 images were sliced into seven classes corresponding to seven *SSA* ranges (0 - 700 $cm^2/g$) (Table 3).

*Table 3: Reflectance values from Landsat TM5 and TM7 and corresponding SSA values. These values were also used to classify the images.*

| ***SSA* ($cm^2/g$)** | 100 | 200 | 300 | 400 | 500 | 600 | 700 |
|---|---|---|---|---|---|---|---|
| **Reflectance TM5** | 0.0223 | 0.0556 | 0.0884 | 0.1211 | 0.1539 | 0.1866 | 0.2193 |
| **Reflectance TM7** | 0.0145 | 0.0418 | 0.0692 | 0.0966 | 0.1239 | 0.1513 | 0.1787 |

In both cases, a good agreement with the field observations was observed also according to the image spectral classification presented in our previous paper (15).

The maps obtained for band TM5 and TM7 are presented in Figures 4 and 5, respectively; the colours correspond to different values of *SSA*. As in Figure 1, fresh snow is presented in red, wind crust in green, while blue represents the snow with faceted crystals. This latter type of snow is mainly located along the glacier, where at that time of the year (early spring) the snow was submitted to metamorphic processes. Sun face surface (white) was not classified nor were shaded areas (black). Also, a good correlation between images data and the '98 snow surveys is found in this case.

## CONCLUSIONS

The results of the classification procedures adopted in this study demonstrate that it is possible to discriminate snow cover with different values of SSA using Landsat infrared images. This was made possible by a good knowledge of the spectral and structural features of the snow targets achieved at the ground. This study also underlines that the range of Landsat infrared bands can be used to describe the distributions of the different types of snow, since at these wavelengths, absorption is very high and the size of the particles is the main factor on the diffusion of light. Given the relations between SSA and snow reflectance in the SWIR wavelengths, it is possible to process remote sensed images in order to describe the spatial distribution of physical characteristics of the snow cover. Applying this methodology it is then possible to obtain SSA maps directly by images, improving the snow metamorphism studies as well as the climate and hydrology studies. This procedure was tested in an area, where climatic conditions are fairly similar in every season and where snow characteristics are spatially constant, thus minimizing the variety of snow types present in a Landsat image. This technique can be exported to other sites at different latitudes. Further improvements in this application will be developed when remote sensing data are acquired in the 900-1300 nm wavelength range and if the temporal resolution of acquisitions on mountain regions is increased.

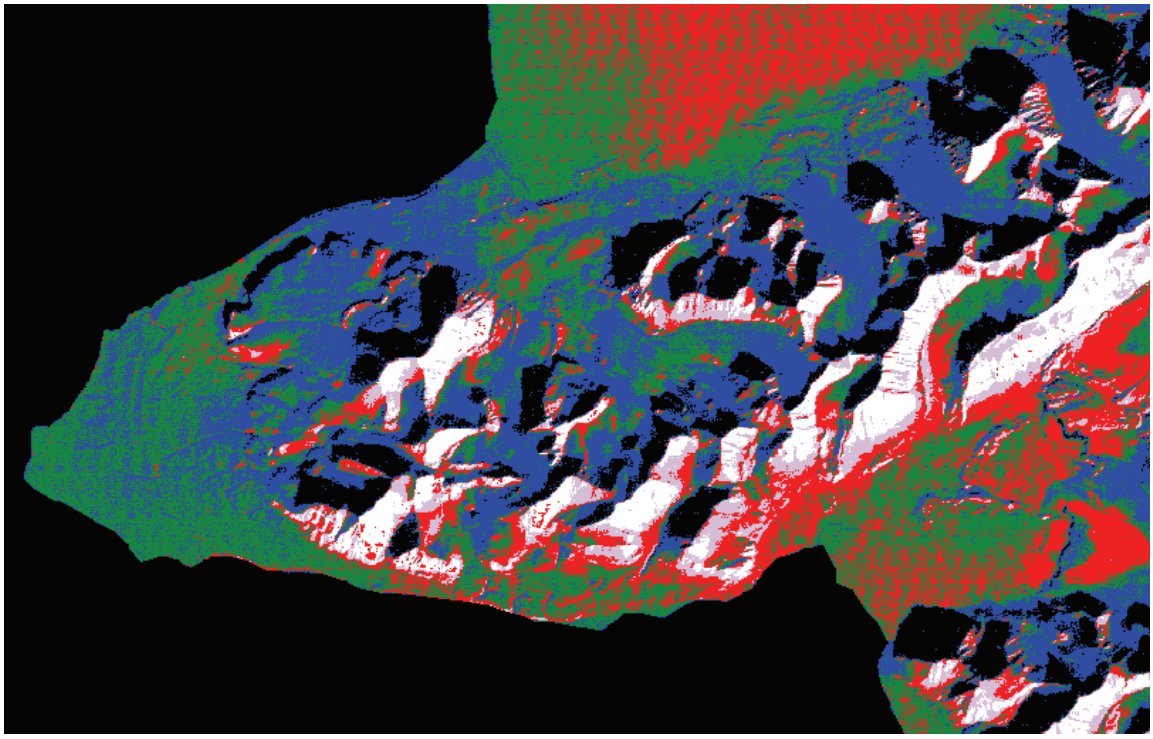

*Figure 4: A Landsat 5 TM5 image classified according to Eq. (1). Colour corresponds to different snow types according to reflectance curves of figure 1 (fresh snow – red, wind crust – green, snow with faceted crystals – blue, unclassified – black, Sun face surface – white).*

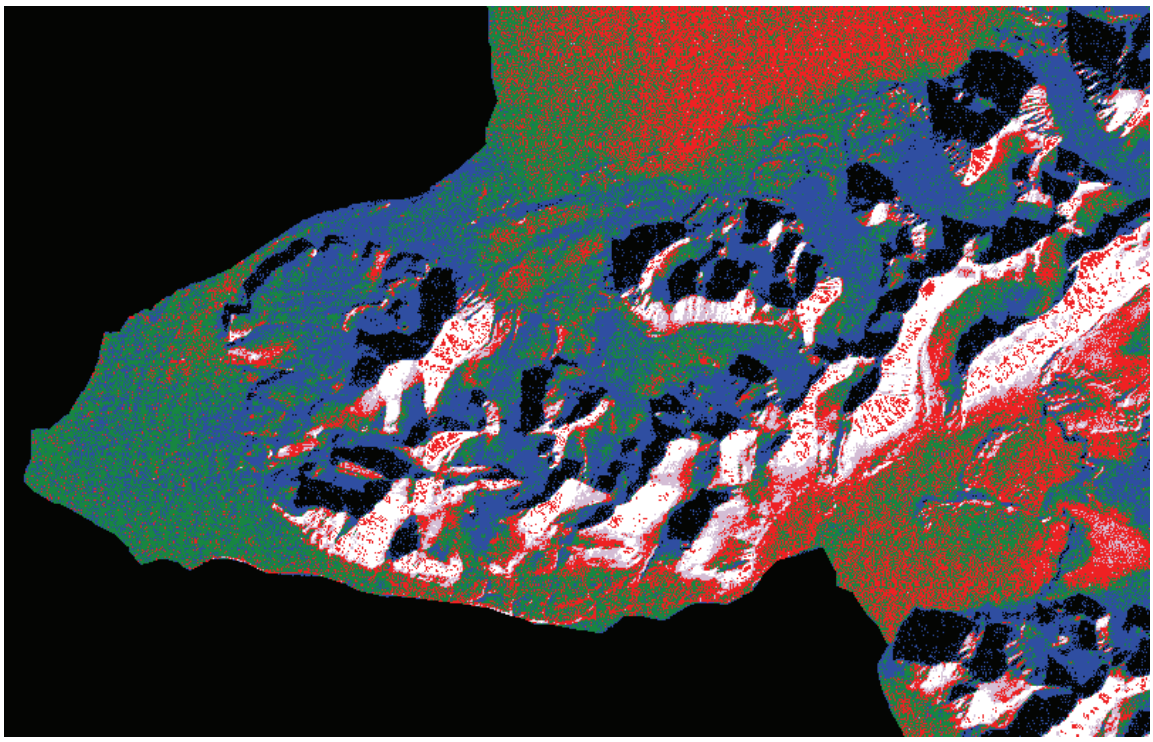

*Figure 5: A Landsat 5 TM7 image classified according to Eq. (2). Colour corresponds to different snow types according to reflectance curves of figure 1 (fresh snow – red, wind crust – green, snow with faceted crystals – blue, unclassified – black, Sun face surface – white).*

**ACKNOWLEDGEMENTS**

The field work of Rosamaria Salvatori in Svalbard was supported by the CNR Arctic Strategic Project, while the field work of Florent Dominé in Svalbard was supported by the French Polar Institute (IPEV) under the POANA program.

**REFERENCES**

1 Painter T H, A D Roberts, R O Green & J Dozier, 1998. The effect of grain size on spectral mixture analysis of snow covered area from AVIRIS data. Remote Sensing of Environment, 65: 320-332

2 Painter T H, J Dozier, A D Roberts, R E Davis & R O Green, 2003. Retrieval of subpixel snow-covered area and grain size from imaging spectrometer data. Remote Sensing of Environment, 85: 64-77

3 Dozier J, 1989. Spectral signature of alpine snow cover from Landsat Thematic Mapper. Remote Sensing of Environment, 28: 9-22

4 Warren S G, 1982. Optical properties of snow. Reviews of Geophysics and Space Physics, 20: 67-89

5 Sergent C, C Leroux, E Pougatch & F Guirado, 1998. Hemispherical–directional reflectance measurements of natural snows in the 0.9–1.45 μm spectral range: comparison with adding–doubling modelling. Annals of Glaciology, 26: 59–63

6 Wiscombe W J & S G Warren, 1980. A model for the spectral albedo of snow. I: pure snow. Journal of Atmospheric Sciences, 37: 2712-2733

7 Neshyba S P, T C Grenfell & S G Warren, 2003. Representation of a nonspherical ice particle by a collection of independent spheres for scattering and absorption of radiation. 2. Hexagonal columns and plates. Journal of Geophysical Research, 108: 4438-4448

8 Dominé F & P B Shepson, 2002. Air–snow interactions and atmospheric chemistry. Science, 297: 1506-1510

9 Dominé F, R Salvatori, L Legagneux, R Salzano, M Fily & R Casacchia, 2006. Correlation between the specific surface area and the short wave infrared (SWIR) reflectance of snow. Cold Regions Science and Technology, 46: 60-68.

10 Casacchia R, R Salvatori, A Cagnati, M Valt & S Ghergo, 2002. Field reflectance of snow/ice covers at Terra Nova Bay Antarctica. International Journal of Remote Sensing, 23: 4563-4667

11 Legagneux L, A Cabanes & F Dominé, 2002. Measurement of the specific surface area of 176 snow samples using methane adsorption at 77 K. Journal of Geophysical Research,107: 4335

12 ITT Corporation, 2007. ENVI 4.3 User's Guide

13 Bourdelles B & M Fily, 1993. Snow grain-size determination from Landsat imagery over Terre Adélie, Antarctica. Annals of Glaciology, 17: 86-92

14 Casacchia R, F Lauta, R Salvatori, A Cagnati, M Valt & J B Orbaek, 2001. Radiometric investigation on different snow covers in Svalbard. Polar Research, 20: 13–22

15 Salvatori R, R Casacchia, A Grignetti, M Valt & A Cagnati, 2005. Snow surface classification in the Western Svalbard Island. In: 31th International Symposium on Remote Sensing of Environment: Global Monitoring for Sustainability and Security (Saint Petersburg, Russia, 20-24 June 2005) http://www.isprs.org/publications/related/ISRSE/html/papers/898.pdf (last date accessed: 21.04.2008)